Variable Galactic Gamma-Ray Sources (VGGRS) VII

Barcelona, 7 May 2025

Galactic runaway O and Be stars found using Gaia DR3 and new stellar bow shocks

Marc Ribó (mribo@ub.edu)

Departament de Física Quàntica i Astrofísica

UNIVERSITAT DE BARCELONA

ICCUB Institut de Ciències del Cosmos

EXCELENCIA MARÍA DE MAEZTU

IEEC

OUTLINE

1. Introduction
2. Runaways with Gaia DR3
3. New bow shocks
4. Search for binaries
5. Conclusions

Introduction

Gamma-ray binaries → excellent laboratories to study particle acceleration, radiation and absorption processes in *periodic* systems **(Bosch-Ramon et al. 2012, 2015, Dubus 2013, 2015, Paredes & Bordas 2019, Bordas 2024, etc.)**.

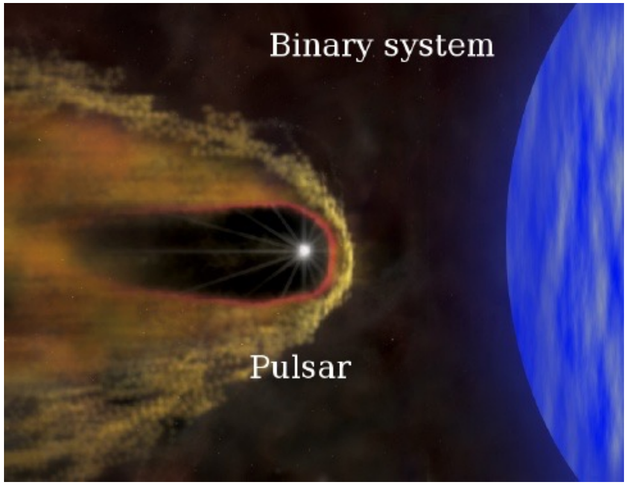

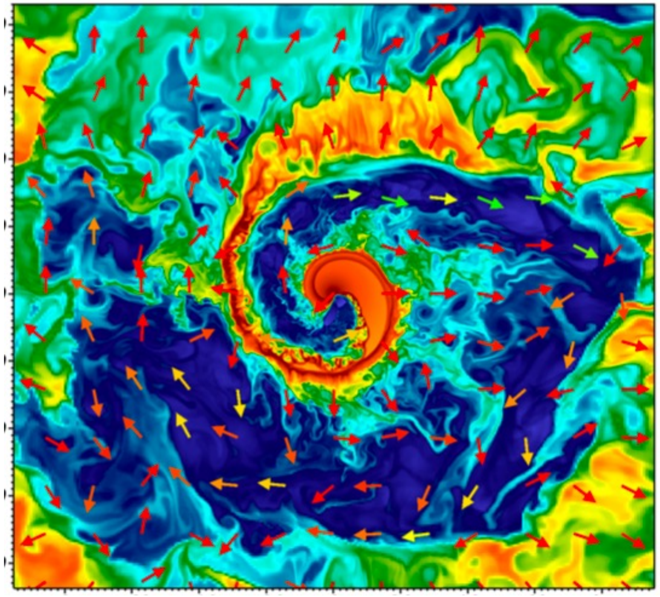

Only **9 systems known**.
O or Be star and a **young non-accreting NS** (at least in 3 cases).

Many **open questions** remain on gamma-ray binaries.
Examples: **What is the real population**? Do we see just the **tip of the iceberg**?

Introduction

3 gamma-ray binaries are runaway binary systems, with a significant peculiar velocity with respect to their environment:

- **LS 5039 (Ribó et al. 2002, Moldón et al. 2012)**.
- **PSR B1259-63 (Miller-Jones et al. 2018)**.
- **1FGL J1018.6-5856 (Marcote et al. 2018)**.

→ Use **runaway massive stars to discover** potential **gamma-ray binaries**.

Ongoing PhD Thesis project of **Mar Carretero-Castrillo** (2021-2025).

Reported partial results in Innsbruck. Today two talks:

- **M. Ribó**: Galactic runaway O and Be stars found using Gaia DR3 and new stellar bow shocks

- **M. Carretero-Castrillo**: O-type runaway binaries with compact objects

Introduction

Scenarios for massive runaway stars:

- **Dynamical ejection scenario** or DES **(Poveda et al. 1967)**.

  Runaway velocity due to dynamical interactions in star clusters.

- **Binary supernova scenario** or BSS **(Blaauw 1961)**.

  Runaway velocity due to supernova explosion of the most evolved star in a binary system

Several studies favor DES over BSS (e.g., Dorigo-Jones et al. 2020).

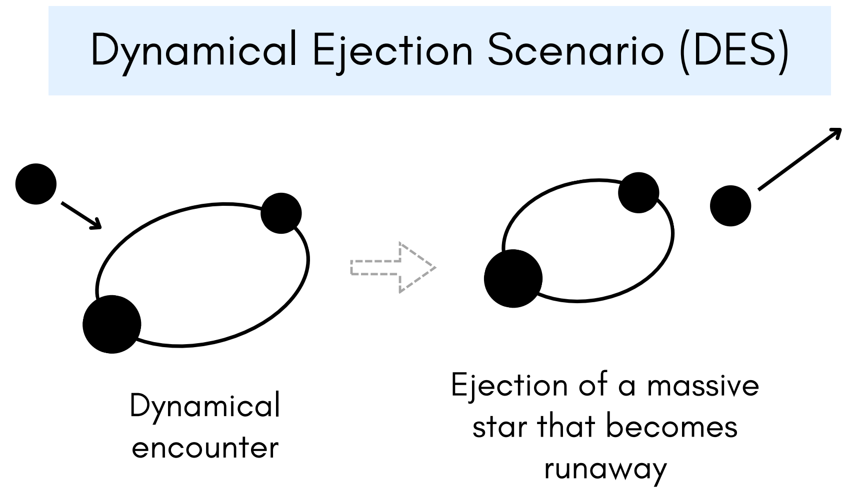

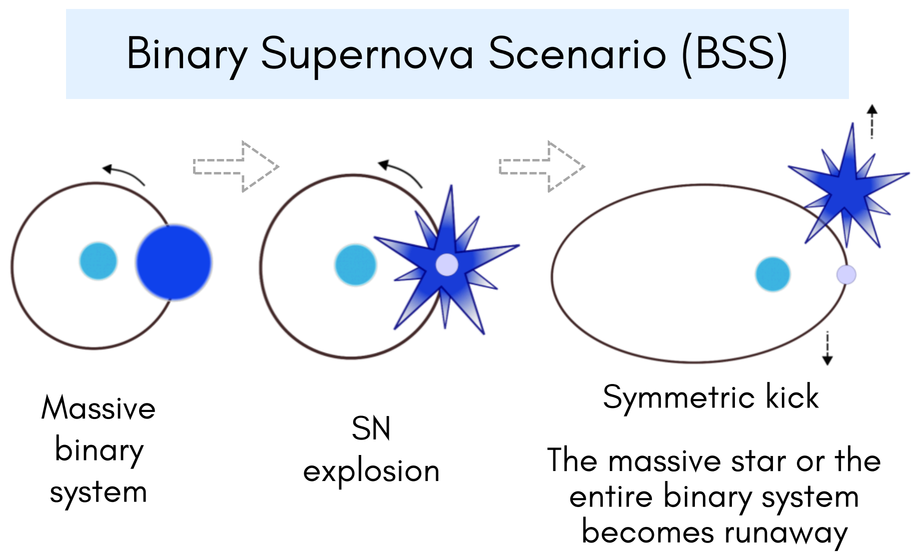

Introduction

Many studies have been conducted in the past to search for massive runaway stars.

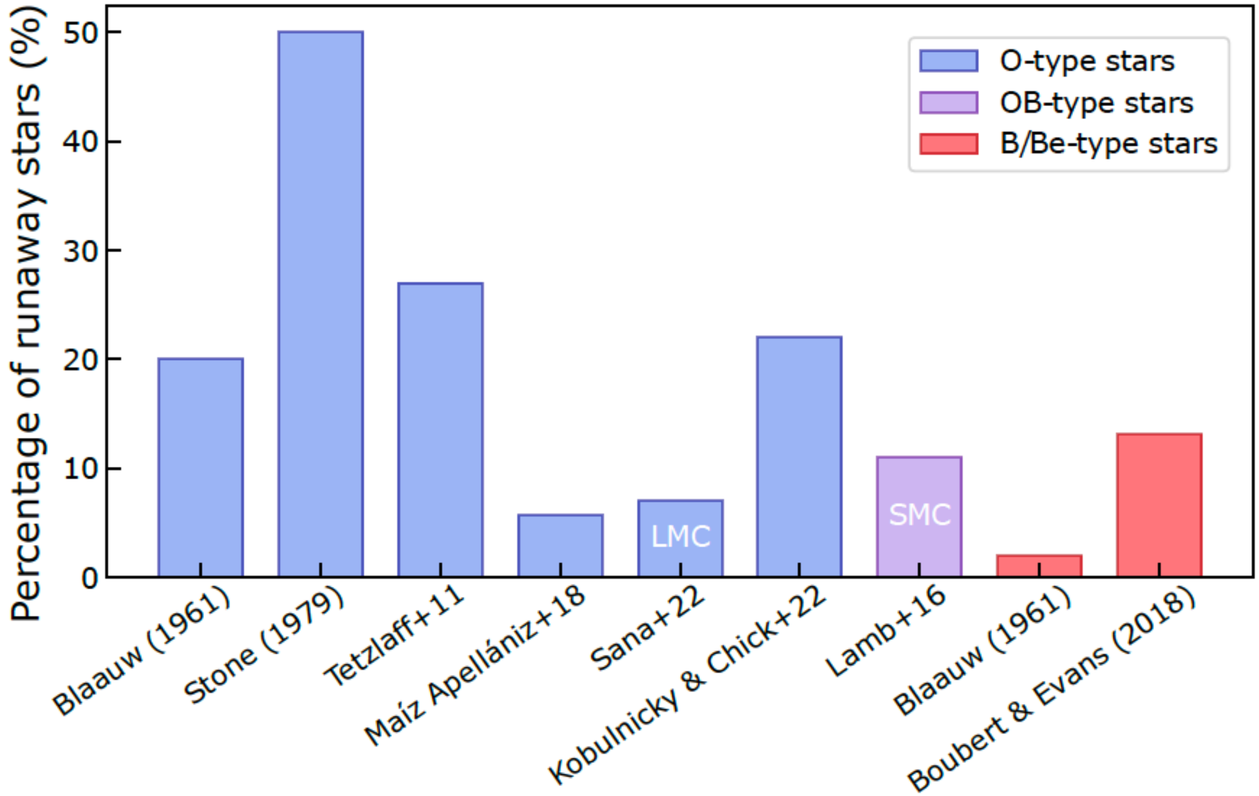

Different methods (and data sets and locations) have been used:

- Proper motions.
- 2-D velocities.
- 3-D velocities.
- Typically using thresholds (25-30 km/s).

The determination of accurate mean **radial velocities** is not straightforward for massive stars (wind contamination, eventual variability, etc.).

Runaways with Gaia DR3

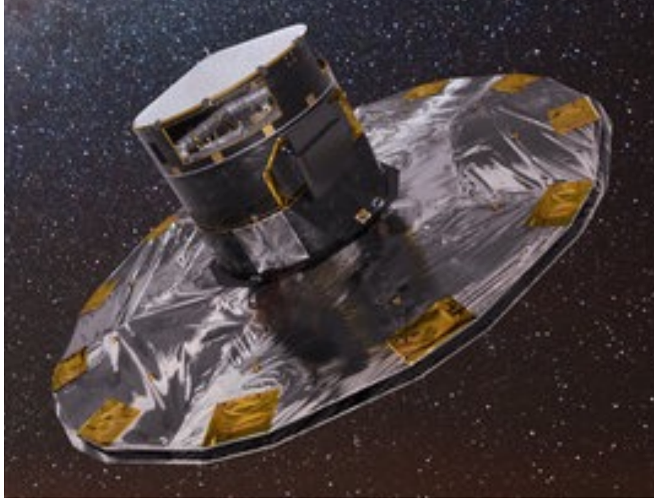

Gaia DR3: accurate **proper motion and distances** !
→ 2-D velocities.

Parallax correction from **Maíz Apellániz (2022)**.

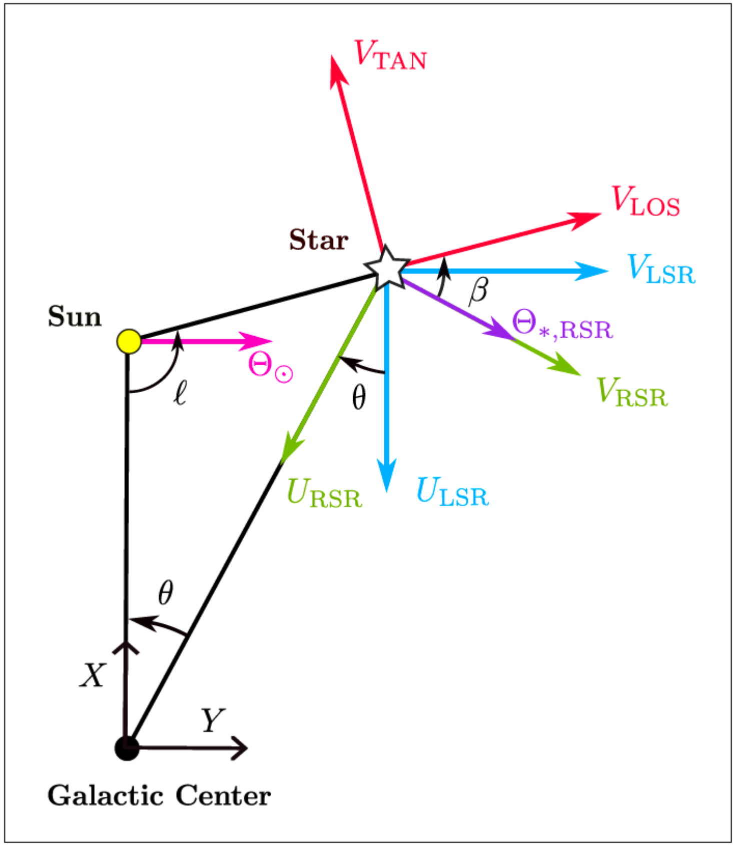

Galactic Rotation curve from model A5 of **Reid (2013)**.

From the Sun to LSR, RSR and rotation.

Runaway stars: deviate 3σ from Galactic Rotation curve. If $E > 1$ → runaway:

$$E = \sqrt{\left(\frac{V_{\mathrm{TAN}} - \mu^{\mathrm{GF}}_{V_{\mathrm{TAN}}}}{3\bar{\sigma}_{V_{\mathrm{TAN}}}}\right)^2 + \left(\frac{W_{\mathrm{RSR}} - \mu^{\mathrm{GF}}_{W_{\mathrm{RSR}}}}{3\bar{\sigma}_{W_{\mathrm{RSR}}}}\right)^2}$$

No threshold.
(Carretero-Castrillo et al. 2023).

Runaways with Gaia DR3

GOSC.

- Galactic O-Star Catalog **(Maíz Apellániz et al. 2004, 2013, 2018)**.
- Available at http://gosc.cab.inta-csic.es
- It contains **643** O and BA stars.
- These authors detected 76 runaway stars (some of them not in GOSC).

BeSS.

- Catalog of Be stars **(Neiner et al. 2011)**.
- Available at http://basebe.obspm.fr/basebe/
- It contains **2330** Be stars.

Runaways with Gaia DR3

GOSC.

- Galactic O-Star Catalog **(Maíz Apellániz et al. 2004, 2013, 2018)**.
- Available at http://gosc.cab.inta-csic.es
- It contains **643** O and BA stars.
- These authors detected 76 runaway stars (some of them not in GOSC).
- After cross-match and quality cuts: GOSC-*Gaia* DR3 catalog of **417** objects.

BeSS.

- Catalog of Be stars **(Neiner et al. 2011)**.
- Available at http://basebe.obspm.fr/basebe/
- It contains **2330** Be stars.
- After cross-match and quality cuts: BeSS-*Gaia* DR3 catalog of **1335** objects.

Runaways with Gaia DR3

GOSC.

- Galactic O-Star Catalog **(Maíz Apellániz et al.**
- Available at http://gosc.cab.inta-csic.es
- It contains **643** O and BA stars.
- These authors detected 76 runaway stars (some
- After cross-match and quality cuts: GOSC-*Gai*

BeSS.

- Catalog of Be stars **(Neiner et al. 2011)**.
- Available at http://basebe.obspm.fr/basebe/
- It contains **2330** Be stars.
- After cross-match and quality cuts: BeSS-*Gaia*

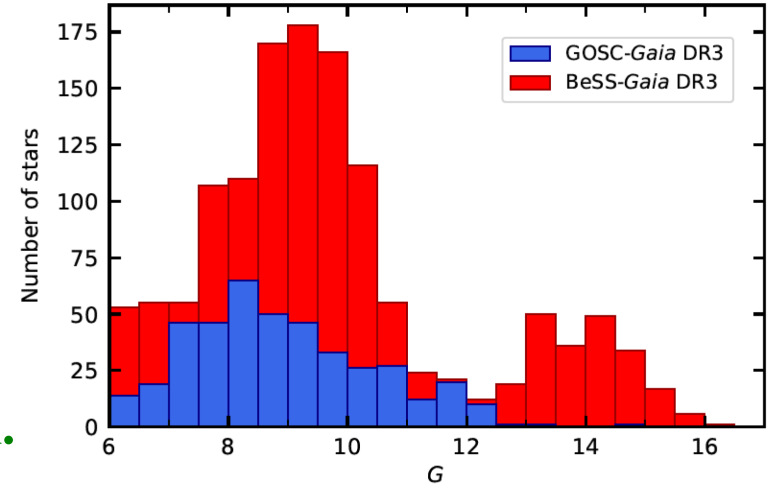

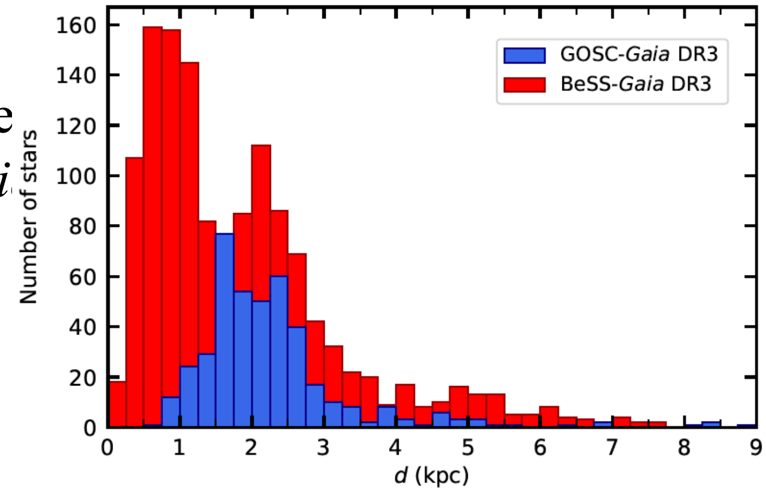

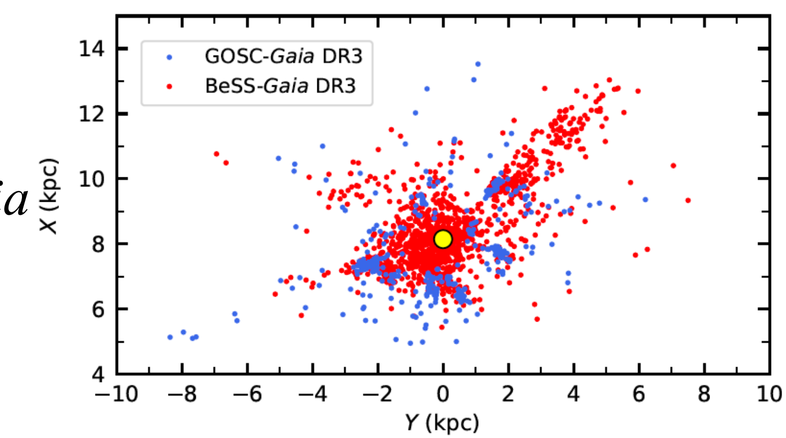

Runaways with Gaia DR3

$$E = \sqrt{\left(\frac{V_{\rm TAN} - \mu^{\rm GF}_{V_{\rm TAN}}}{3\bar{\sigma}_{V_{\rm TAN}}}\right)^2 + \left(\frac{W_{\rm RSR} - \mu^{\rm GF}_{W_{\rm RSR}}}{3\bar{\sigma}_{W_{\rm RSR}}}\right)^2}$$

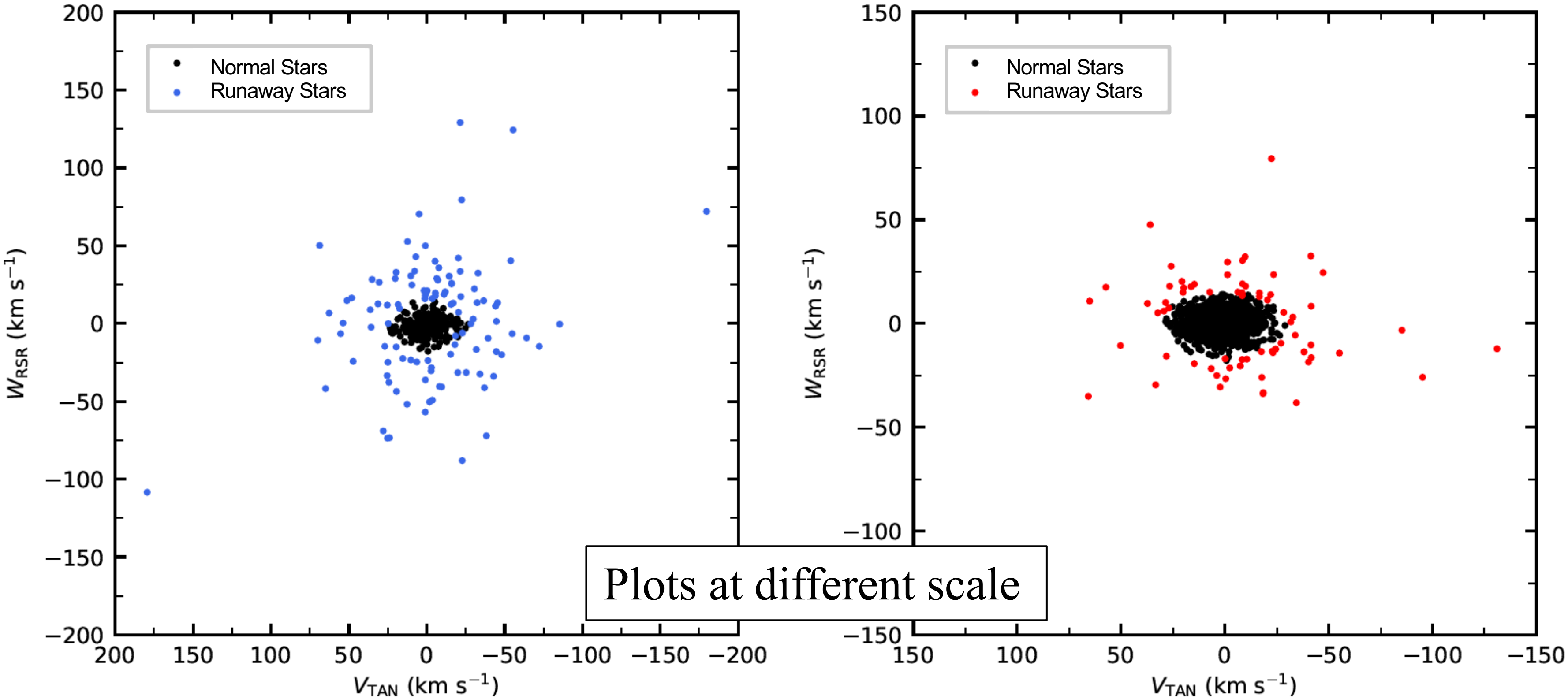

Plots at different scale

GOSC-*Gaia* DR3:

- **106 runaways, 42 new**.
- **16-210 km/s** (no threshold).
- Runaways fraction: **25.4%**.

BeSS-*Gaia* DR3:

- **69 runaways, 47 new**.
- **16-132 km/s** (no threshold).
- Runaways fraction: **5.2%**.

(Carretero-Castrillo et al. 2023).

Runaways with Gaia DR3

$$E = \sqrt{\left(\frac{V_{\mathrm{TAN}} - \mu^{\mathrm{GF}}_{V_{\mathrm{TAN}}}}{3\bar{\sigma}_{V_{\mathrm{TAN}}}}\right)^2 + \left(\frac{W_{\mathrm{RSR}} - \mu^{\mathrm{GF}}_{W_{\mathrm{RSR}}}}{3\bar{\sigma}_{W_{\mathrm{RSR}}}}\right)^2}$$

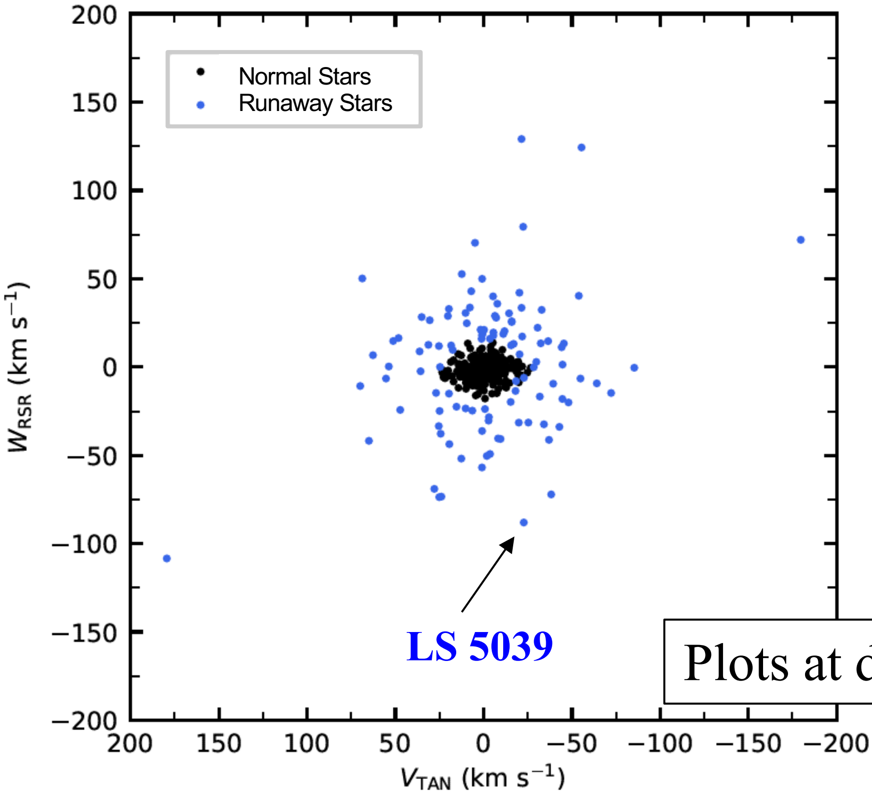

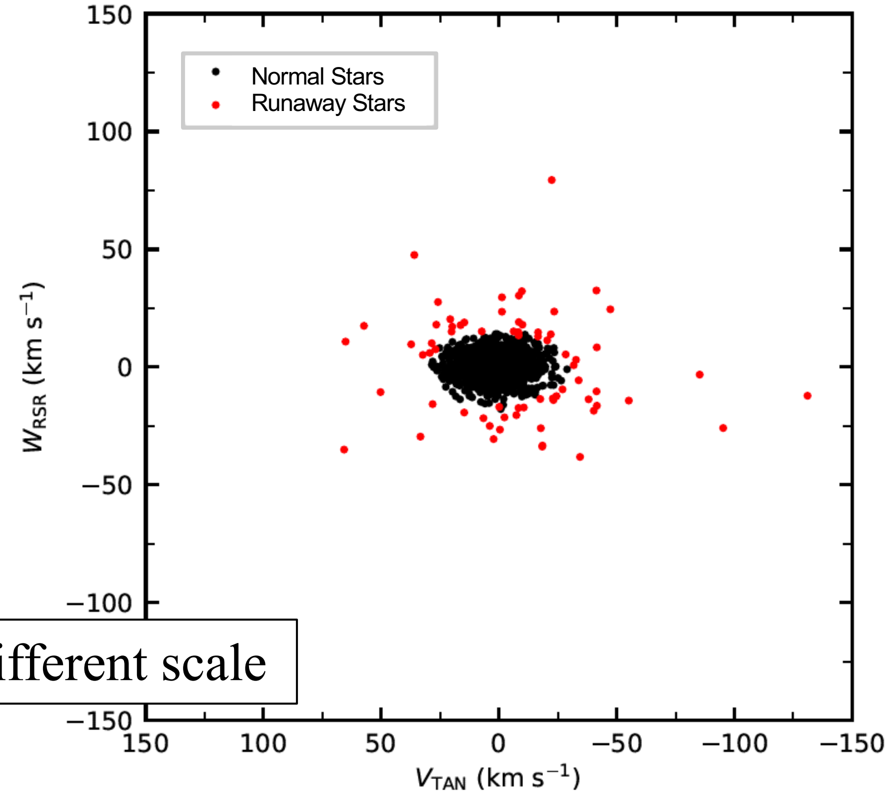

Plots at different scale

GOSC-*Gaia* DR3:

- **106 runaways, 42 new**.
- **16-210 km/s** (no threshold).
- Runaways fraction: **25.4%**.

BeSS-*Gaia* DR3:

- **69 runaways, 47 new**.
- **16-132 km/s** (no threshold).
- Runaways fraction: **5.2%**.

(Carretero-Castrillo et al. 2023).

Runaways with Gaia DR3

The **runaway percentage decreases as we move to later spectral types** (noted in previous studies, e.g., **Dorigo-Jones et al. 2020**).

We obtained a **factor of 5 between O and Be runaway stars**:
reinforces **dominance of DES vs. BSS (Carretero-Castrillo et al. 2023)**.

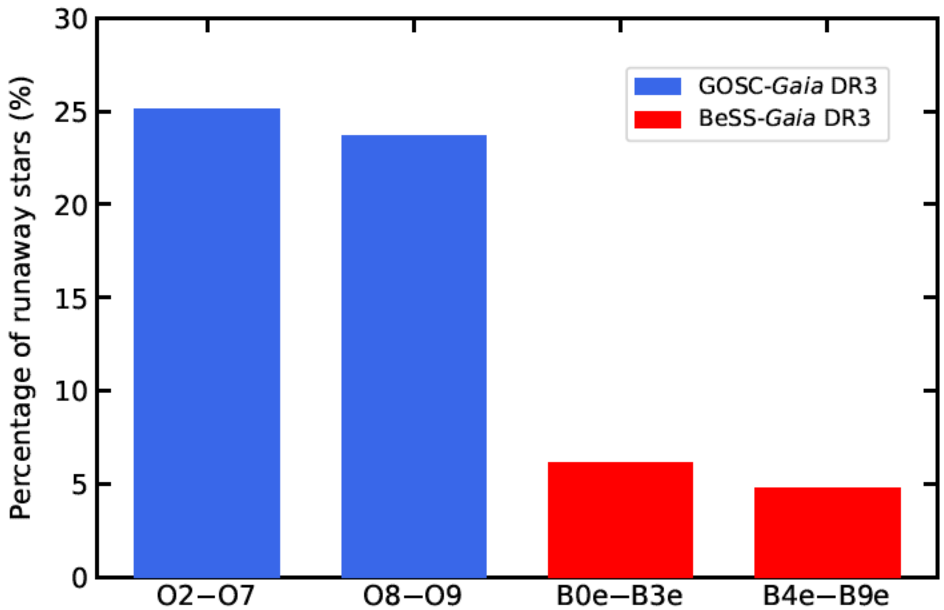

Spectral Type	Stars	Runaway Stars	
	#	#	%
O2–O7	199	50	25.1
O8–O9	194	46	23.7
B0e–B3e	585	36	6.2
B4e–B9e	482	23	4.8
O8–B1e	420	62	14.8

New bow shocks

Accumulation of **ISM matter** as a runaway star with a **powerful wind** sweeps up and **heats** the surrounding gas and dust, which **emits mostly in IR**.

If the star's velocity is **supersonic**, a strong bow shock takes place → promising places for the **acceleration of relativistic particles**.

Face on bow shocks may present a spherical or **bubble shape**.

Bow shocks studies are relevant to constrain **ISM density**, particle acceleration, and non-thermal radio emission.

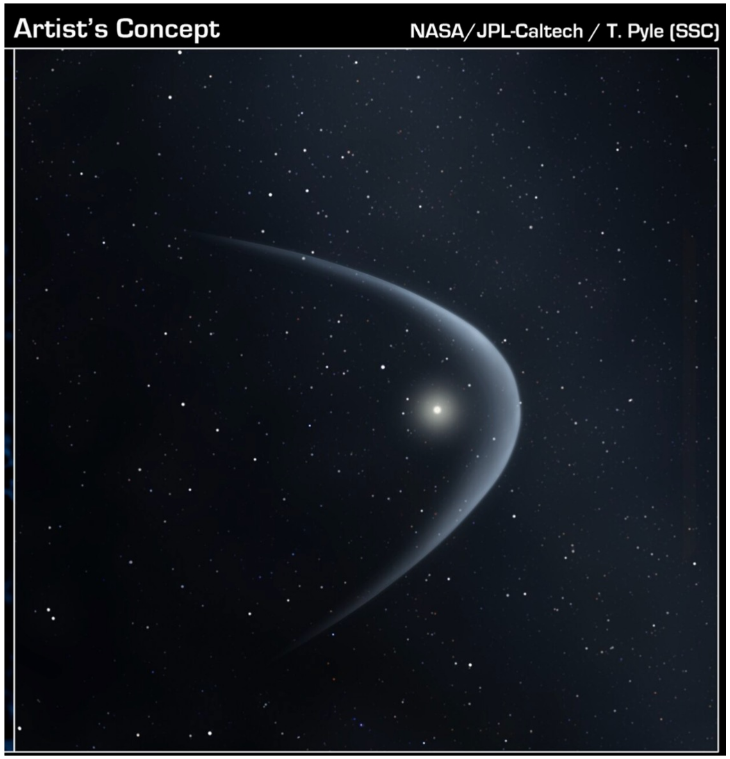

(Noriega-Crespo et al. 1997, Benaglia et al. 2010, Del Valle & Romero 2012, Peri et al. 2012, 2015, Del Palacio et al. 2018, Benaglia 2024).

New bow shocks

We searched the **Wide-field Infrared Survey Explorer** (WISE) around the positions of the runaways in **Carretero-Castrillo et al. (2023)**.

We used **W4 images** at 22 μm.

We **corrected the Gaia DR3 proper motions** for the ISM motion caused by Galactic rotation **(Comerón & Pasquali 2007)**.

Criteria for bow shock or bubble candidate classification:

1. The presence of a bow shock-like or bubble-like structure **around the runaway star**
2. Arc-shaped structure/or the rim of the bubble in the **direction of the runaway star's corrected proper motion**

New bow shocks

Results:

New bow shocks or bubbles:

9 new bow shock candidates
3 new bubble candidates
1 mixed structured candidate

17 known bow shock or bubble candidates (but discarded one):

**(Peri et al. 2012, 2015, Kobulnicky et al. 2016 ,
Maíz Apellániz et al. 2018, Bodensteiner et al. 2018)**

Miscellaneous

62 miscellaneous structures with IR emission around the runaway star

New bow shocks

Band	Wavelength	Resolution
W1	3.4 µm	6.1"
W2	4.6 µm	6.4"
W3	12 µm	6.5"
W4	22 µm	12"

RGB images using W4, W3 and W2 from WISE:

 Corrected Gaia DR3 proper motion (2' size).

 Gaia DR3 proper motion (2' size).

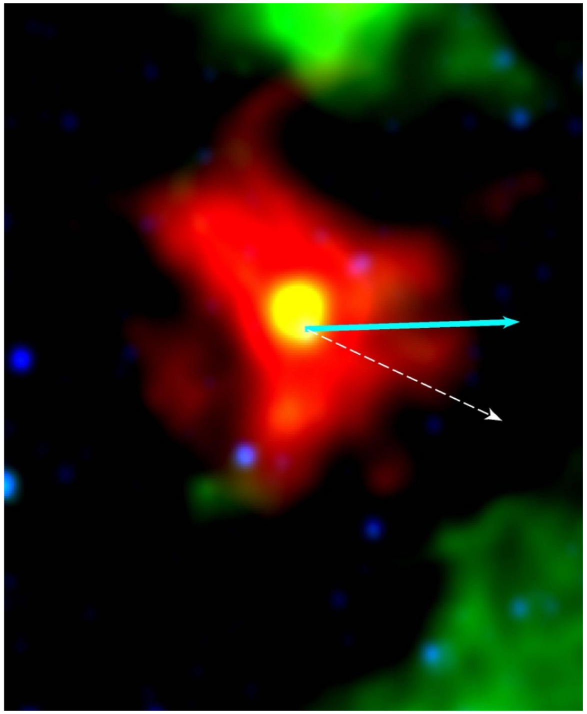

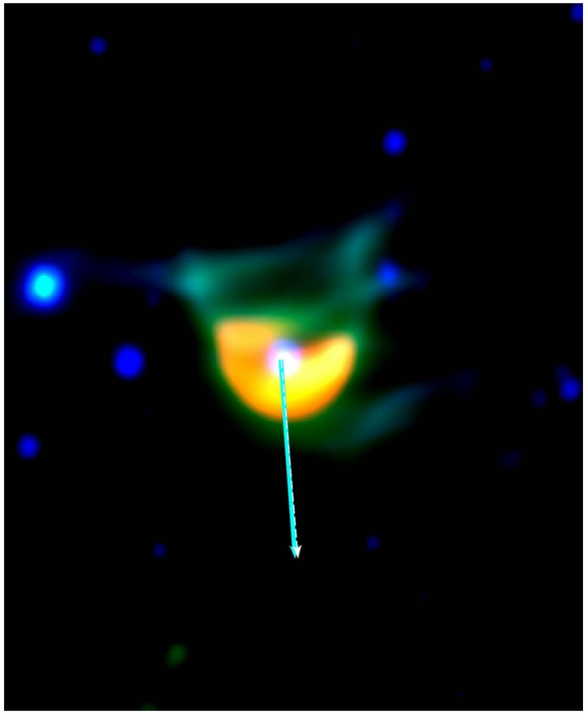

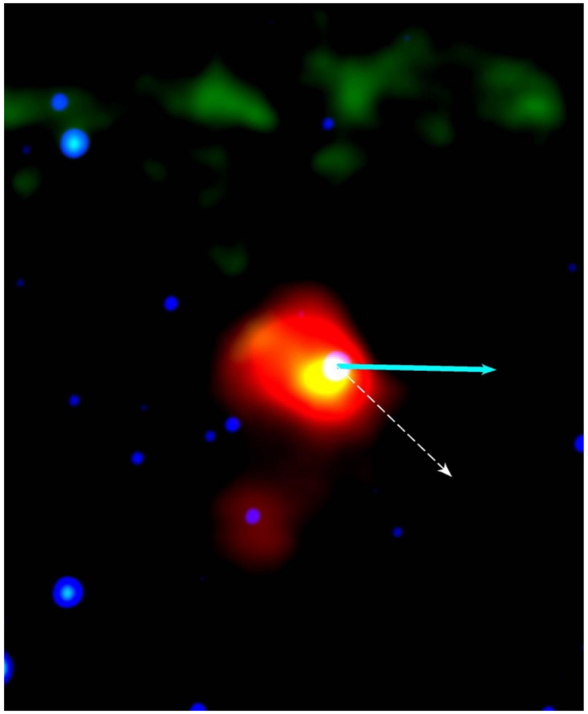

New bow shocks

Geometrical characterization of W4 images and ISM density.

Median values of the projected distances:

Stand-off distance ***R***		Width *w*		Length **ℓ**	
21″	0.32 pc	74″	0.76 pc	175″	1.96 pc

$$R_0 = \sqrt{\frac{\dot{M} v_\infty}{4\pi\rho_a {V_{\rm PEC}^{\rm 3D}}^2}} \Rightarrow n_{\rm ISM}$$

(Wilkin 1996, Martins et al. 2005,
Vink & Sander (2021)

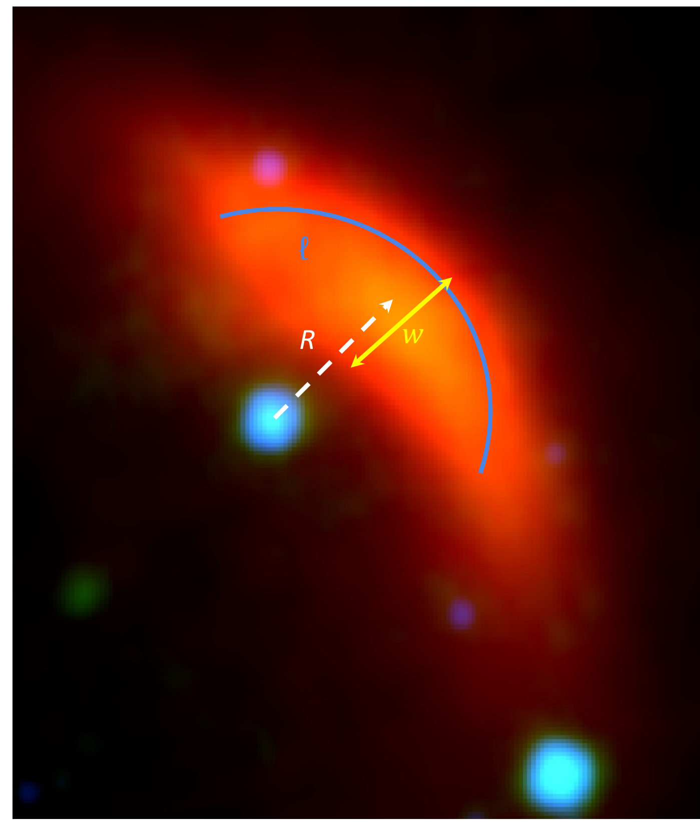

ISM densities at the bow shock position:
0.3 to 198.6 cm^{-3}, with a **median of ~5 cm^{-3}**.

Useful for other studies at those positions
(stellar formation studies, radiation processes in these regions, ...).

New bow shocks

Radio surveys: NVSS, VLASS, and RACS (mid and low)
Two bow shocks present **radio emission but not as clear counterparts**.
Color: WISE 4 (22μm). **Contours**: RACS low (887.5 MHz).

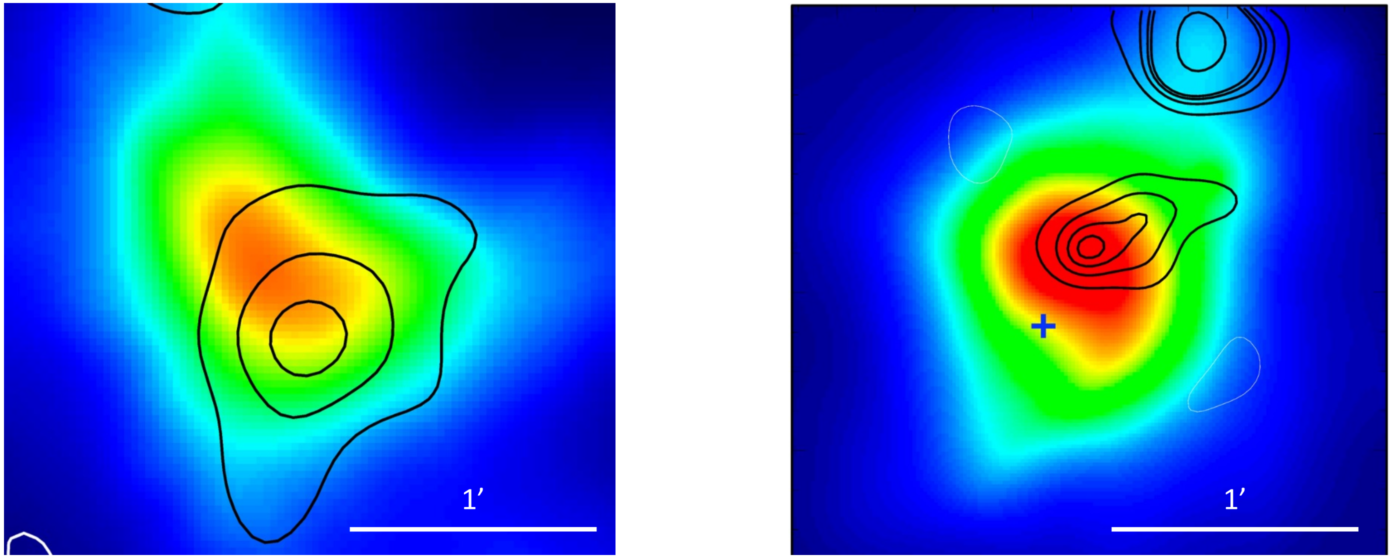

Two others show hints of radio emission.
We study the radio detectability of the sources under thermal and non-thermal scenarios: 2 sources could be compatible with the non-thermal one.
(Carretero-Castrillo et al. 2025).

New bow shocks

VLA observations of 8 of the runaways at 2–4 GHz in C configuration to discover:

- ➢ radio emitting bow shocks
- ➢ radio emission from the massive stars

We only detected a known HII region (S206) around one of the sources.

More sensitive radio observations of these sources could eventually unveil new radio counterparts.

(Carretero-Castrillo 2025, PhD Thesis, to be submitted).

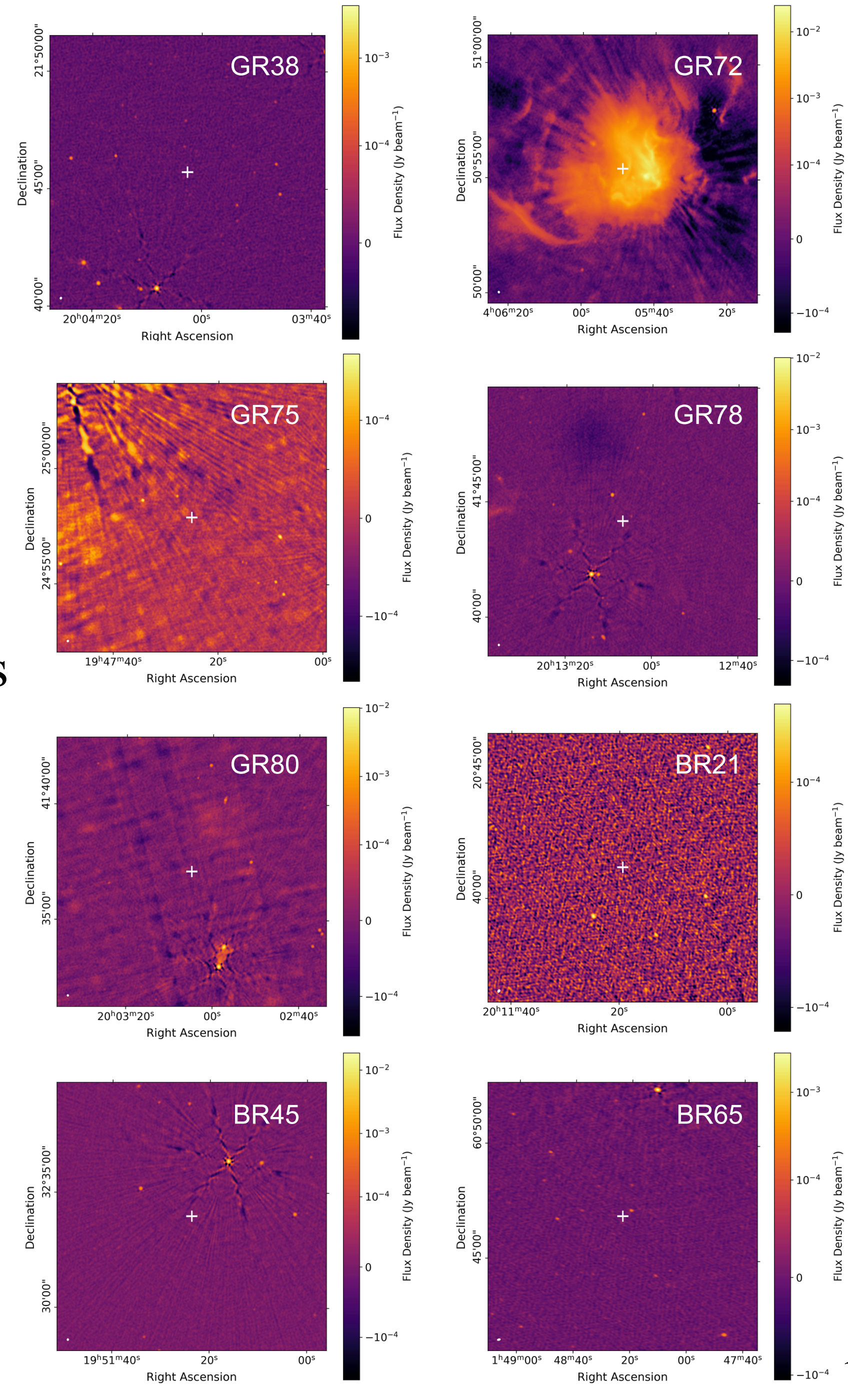

Search for binaries

Multiwavelength data + radial velocities
(radio, X-rays, HE and VHE gamma rays)

→ **High-energy binary systems**

Conclusions

- Runaways with Gaia DR3: there are **many (and new) O and Be runaways and walkaways**; some of them could be **potential gamma-ray binaries**.

  Galactic runaway O and Be stars found using Gaia DR3
  Carretero-Castrillo, Ribó & Paredes 2023, A&A, 679, A109

- New bow shocks: a few **additional bow shock candidates** have been found, some of them with **hints of radio emission, but no clear counterpart**.

  New stellar bow shocks and bubbles found around runaway stars
  Carretero-Castrillo, Benaglia, Paredes & Ribó 2025, A&A, 694, A250

- Search for binaries (plus more on the scenarios): next talk…

  An observational study of rotation and binarity of Galactic O runaway stars, Carretero-Castrillo, Ribó, Paredes, Holgado, Martínez-Sebastián & Simón-Díaz, to be submitted to A&A

Backup

Backup

System	HE	VHE	Star	CO	P_{orbit}
LS 5039	Y	Y	ON6.5 V	?	3.9 d
LMC P3	Y	Y	O5 III	?	10.3 d
4FGL J1405.1-6119	Y	-	O6.5 III	?	13.7 d
1FGL J1018.6-5856	Y	Y	O6 V	?	16.5 d
HESS J1832-093	Y	Y	O6 V	?	86.3 d
LS I +61 303	Y	Y	B0 Ve	PSR (269 ms)	26.5 d
HESS J0632+057	Y	Y	B0 Vpe	?	317 d
PSR B1259-63	Y	Y	O9.5 Ve	PSR (47.7 ms)	~3.4 yr
PSR J2032+4127	~Y	Y	B0 Vpe	PSR (143 ms)	~50 yr

Basically: O6 III-V stars and B0 Ve stars.

Backup

Quality Cut	GOSC Stars		BeSS Stars	
	#	%	#	%
Stars in pairs with same Gaia `source_id`	6	1.0	2	0.1
Non 5- or 6-parameter solution	9	1.5	29	1.6
$G < 6$	46	7.7	159	8.8
`visibility_periods_used` < 10	5	0.8	16	0.9
$\sigma_{\rm ext}/\varpi_{\rm c} > 0.2$	72	12.0	145	8.0
Negative parallax	5	0.8	18	1.0
RUWE > 1.35	116	19.4	282	15.6
All cuts	175	29.3	472	26.1

Backup

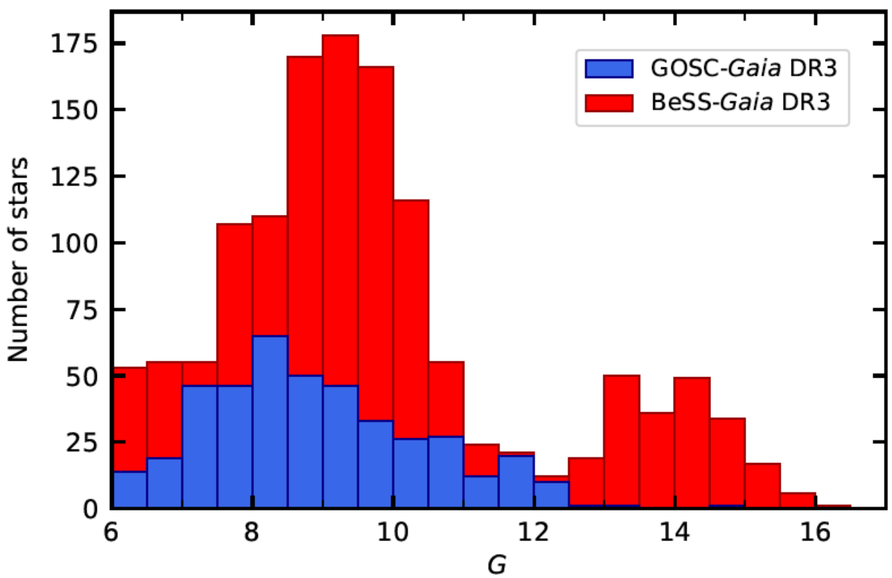

Fig. 1. Histogram of the G magnitudes for GOSC-*Gaia* DR3 stars in blue and BeSS-*Gaia* DR3 stars in red, with a bin size of 0.5 magnitudes.

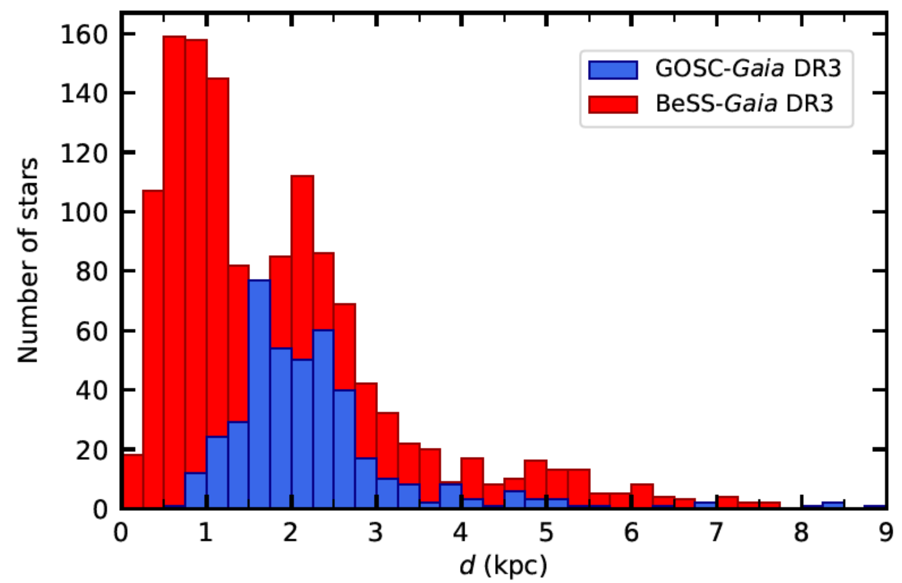

Fig. 2. Histogram of the distances to the Sun of GOSC-*Gaia* DR3 stars in blue and of BeSS-*Gaia* DR3 stars in red, with a bin size of 0.25 kpc.

Backup

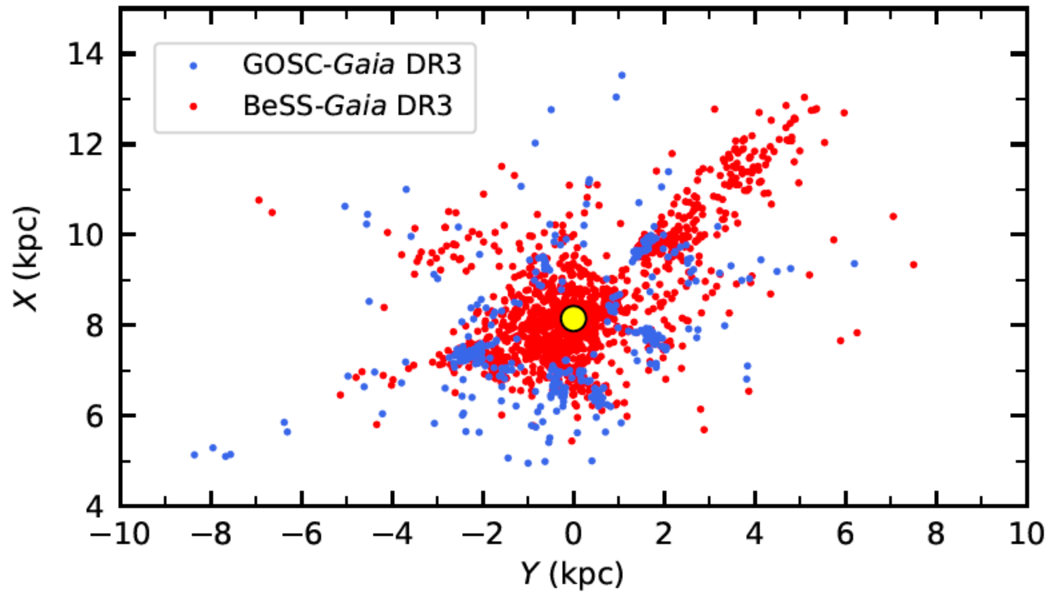

Fig. 3. Galactocentric XY coordinates. The coordinates of the GOSC-*Gaia* DR3 stars are shown in blue, and those of the BeSS-*Gaia* DR3 stars are plotted in red. The position of the Sun is marked with a yellow circle at $(X, Y) = (8.15, 0)$ kpc. The Galactic center is located at $(0, 0)$ kpc.

Backup

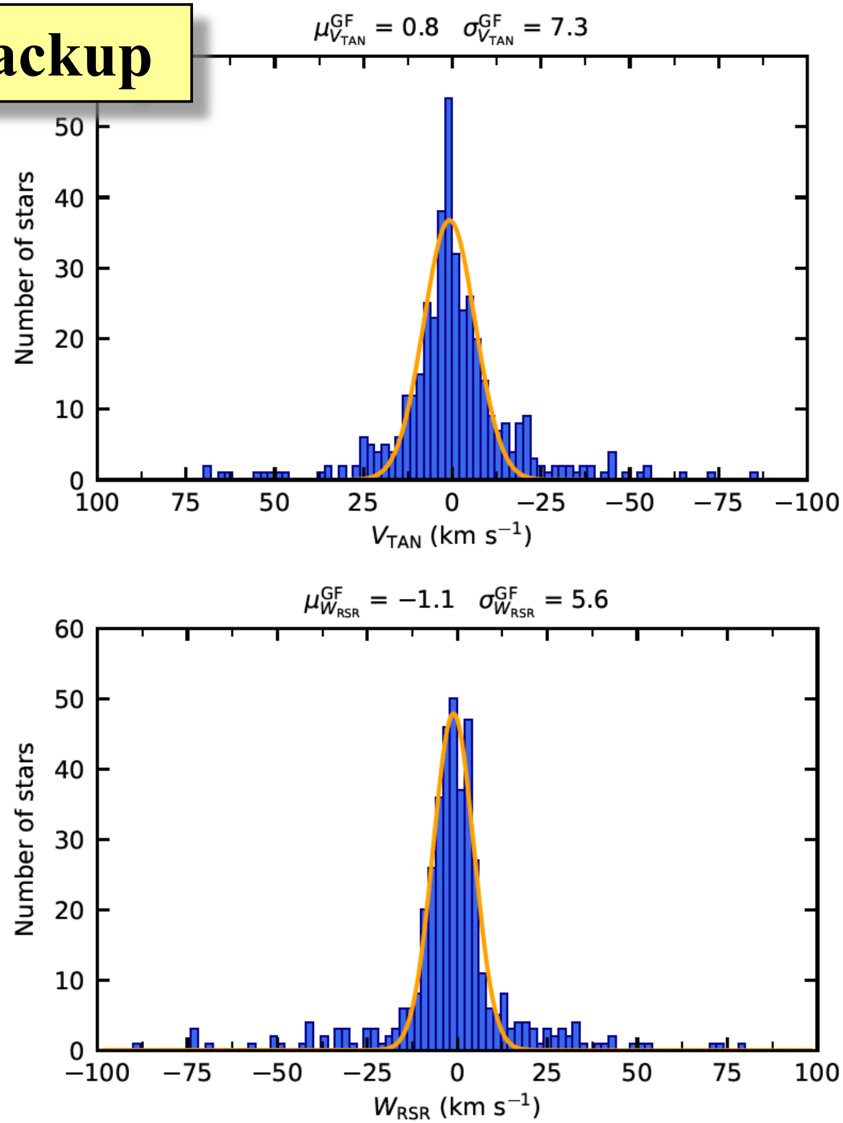

Fig. 5. Distributions of the V_{TAN} and W_{RSR} velocities for the GOSC-*Gaia* DR3 stars. The histograms have a bin size of 2 km s^{-1}. The orange lines represent Gaussian functions (GF) fitted to the data, whose means and standard deviations in km s^{-1} are quoted above the panels. The abscissa ranges have been limited to ±100 km s^{-1}. *Top*: histogram of the V_{TAN} velocities. *Bottom*: histogram of the W_{RSR} velocities.

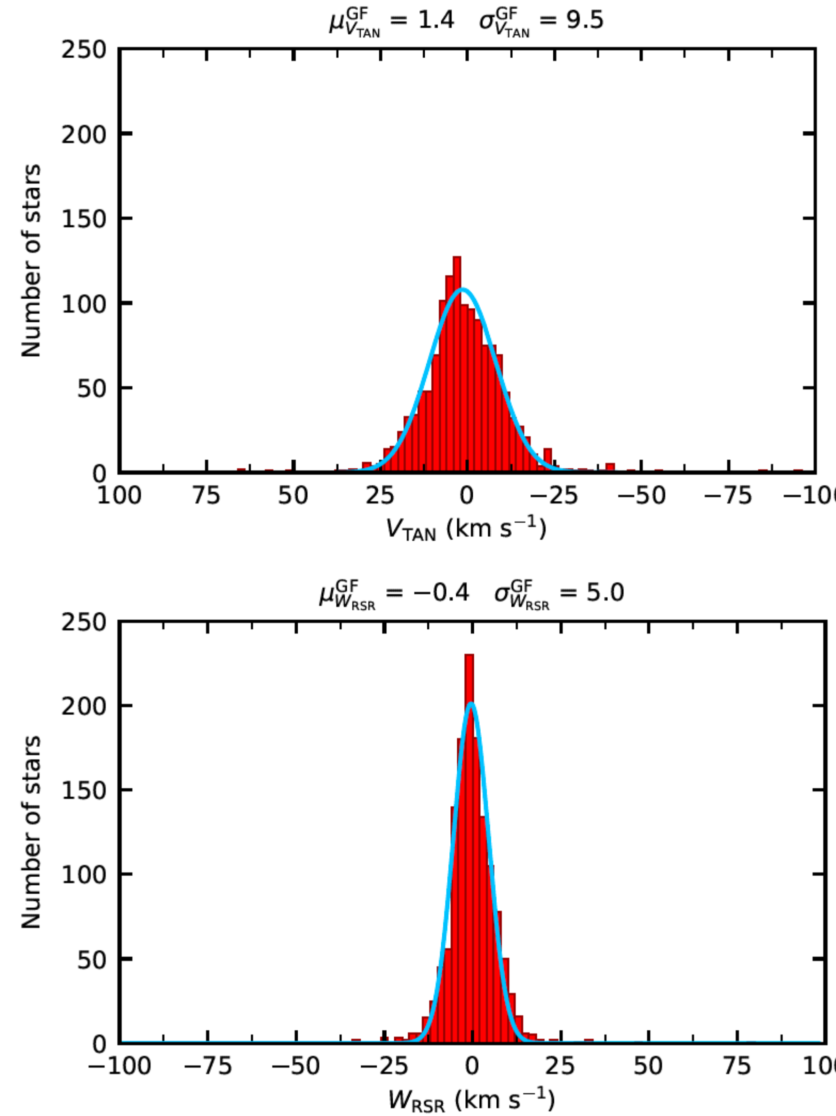

Fig. 6. Same as Fig. 5 but for the BeSS-*Gaia* DR3 stars and with the Gaussian functions fitted to the data shown in blue.

Backup

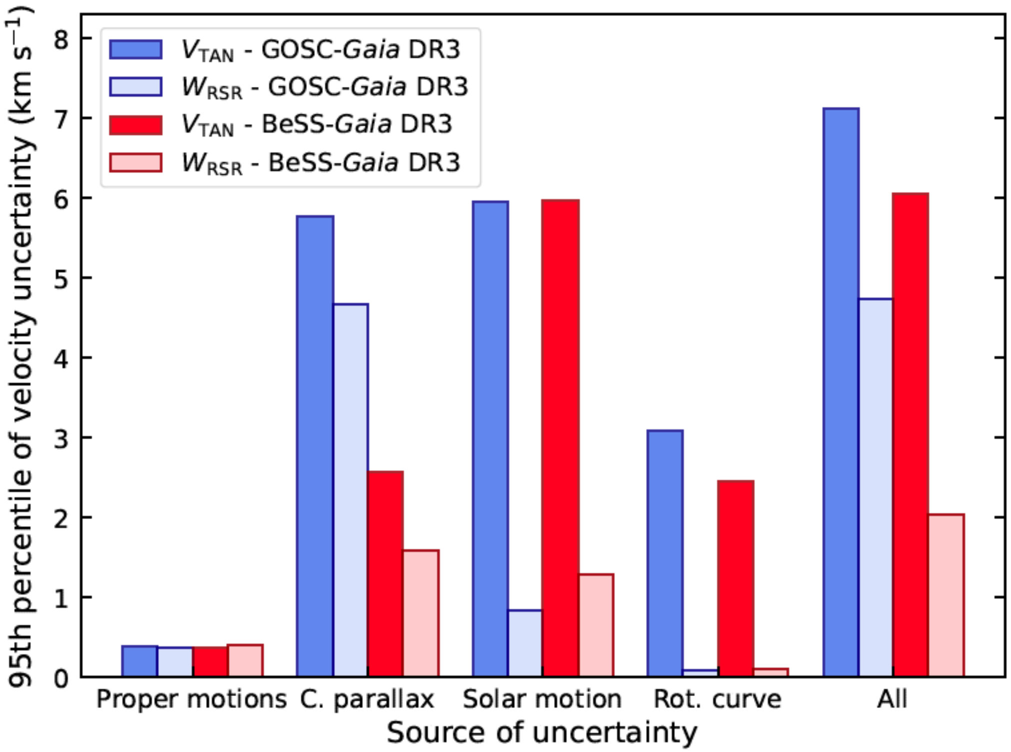

Fig. 7. Ninety-fifth percentile of the V_{TAN} and W_{RSR} velocity uncertainties for different sources of uncertainty, and considering all the uncertainties together, for GOSC-*Gaia* DR3 stars in blue and BeSS-*Gaia* DR3 stars in red.

Backup

Table 1. Means and standard deviations of different distributions for the field stars after clipping.

Catalog	Stars #	Field stars #	$\mu^{GF}_{V_{TAN}} \pm \sigma^{GF}_{V_{TAN}}$ (km s^{-1})	$\mu^{GF}_{W_{RSR}} \pm \sigma^{GF}_{W_{RSR}}$ (km s^{-1})	$\mu_Z \pm \sigma_Z$ (kpc)	$\mu_b \pm \sigma_b$ (°)
GOSC-*Gaia* DR3	417	311	1.0 ± 6.6	-1.0 ± 5.3	-0.01 ± 0.07	-0.1 ± 2.0
BeSS-*Gaia* DR3	1335	1266	1.6 ± 9.3	-0.5 ± 4.9	-0.01 ± 0.11	-1.0 ± 6.5
GOSC-*Gaia* DR3 ($d < 2$ kpc)	197	145	-0.1 ± 5.0	1.4 ± 4.2	0.02 ± 0.04	0.6 ± 2.1
BeSS-*Gaia* DR3 ($d < 2$ kpc)	831	793	0.6 ± 9.7	-0.4 ± 5.1	-0.02 ± 0.10	-1.5 ± 8.2

Table 2. Means and standard deviations of different distributions for the runaway stars after clipping.

Catalog	Stars #	Runaway stars #	$\mu_{V_{TAN}} \pm \sigma_{V_{TAN}}$ (km s^{-1})	$\mu_{W_{RSR}} \pm \sigma_{W_{RSR}}$ (km s^{-1})	$\mu_Z \pm \sigma_Z$ (kpc)	$\mu_b \pm \sigma_b$ (°)
GOSC-*Gaia* DR3	417	106	-3.1 ± 39.7	1.1 ± 38.7	0.01 ± 0.19	0.2 ± 4.3
BeSS-*Gaia* DR3	1335	69	-7.7 ± 34.6	1.0 ± 22.3	-0.09 ± 0.66	-3.4 ± 21.2
GOSC-*Gaia* DR3 ($d < 2$ kpc)	197	52	-3.9 ± 28.6	-0.6 ± 32.3	0.00 ± 0.11	-0.1 ± 4.1
BeSS-*Gaia* DR3 ($d < 2$ kpc)	831	38	-5.7 ± 33.0	1.8 ± 22.9	-0.06 ± 0.40	-3.2 ± 22.1

Backup

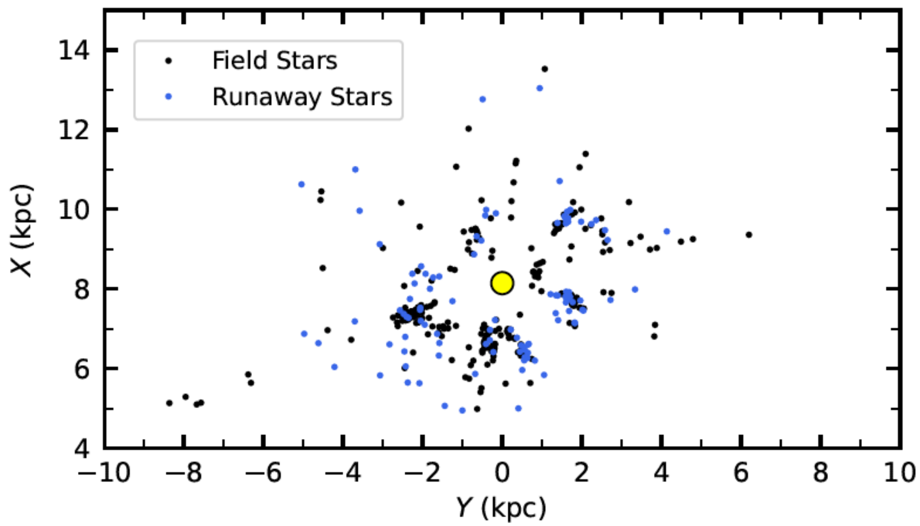

Fig. 10. Galactocentric XY coordinates for the GOSC-*Gaia* DR3 stars. Field stars are depicted in black, and runaway stars are shown in blue. The position of the Sun is marked with a yellow circle at $(X, Y) = (8.15, 0)$ kpc.

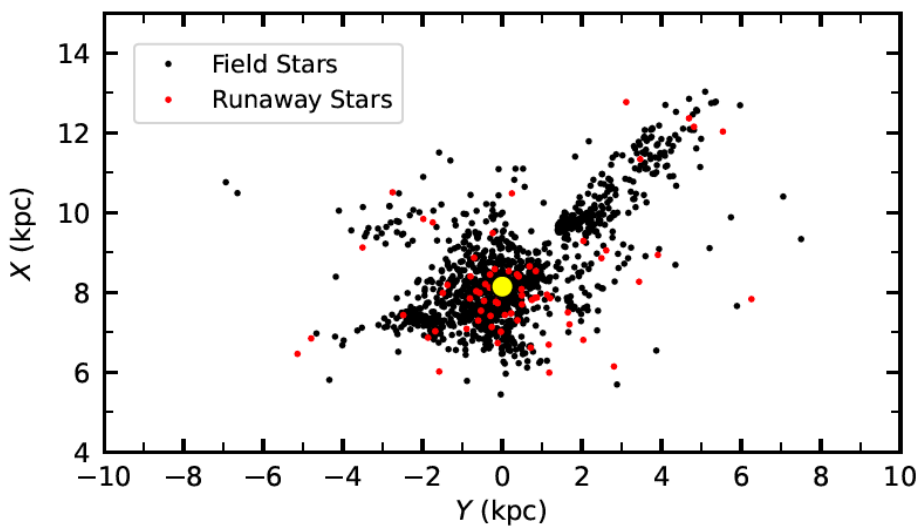

Fig. 11. Same as Fig. 10 for the BeSS-*Gaia* DR3 stars. Field stars are depicted in black, and runaway stars are shown in red.

Backup

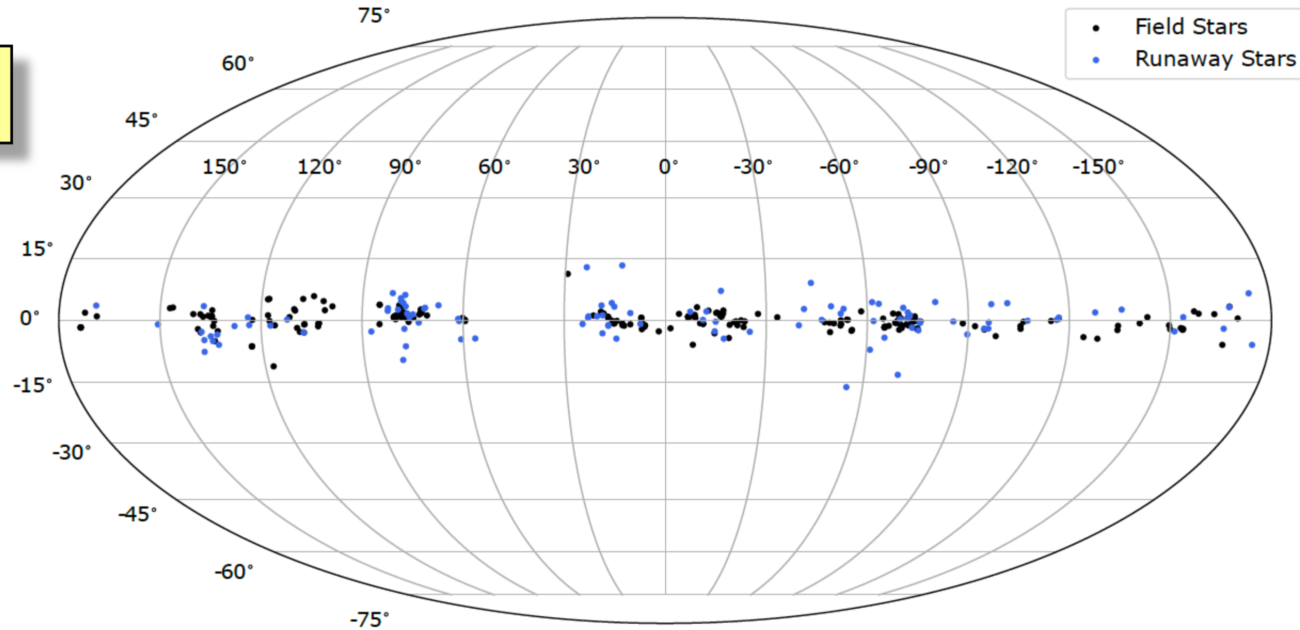

Fig. 12. Galactic (l, b) coordinates for GOSC-*Gaia* DR3 stars. Field stars are depicted in black, and runaway stars are shown in blue.

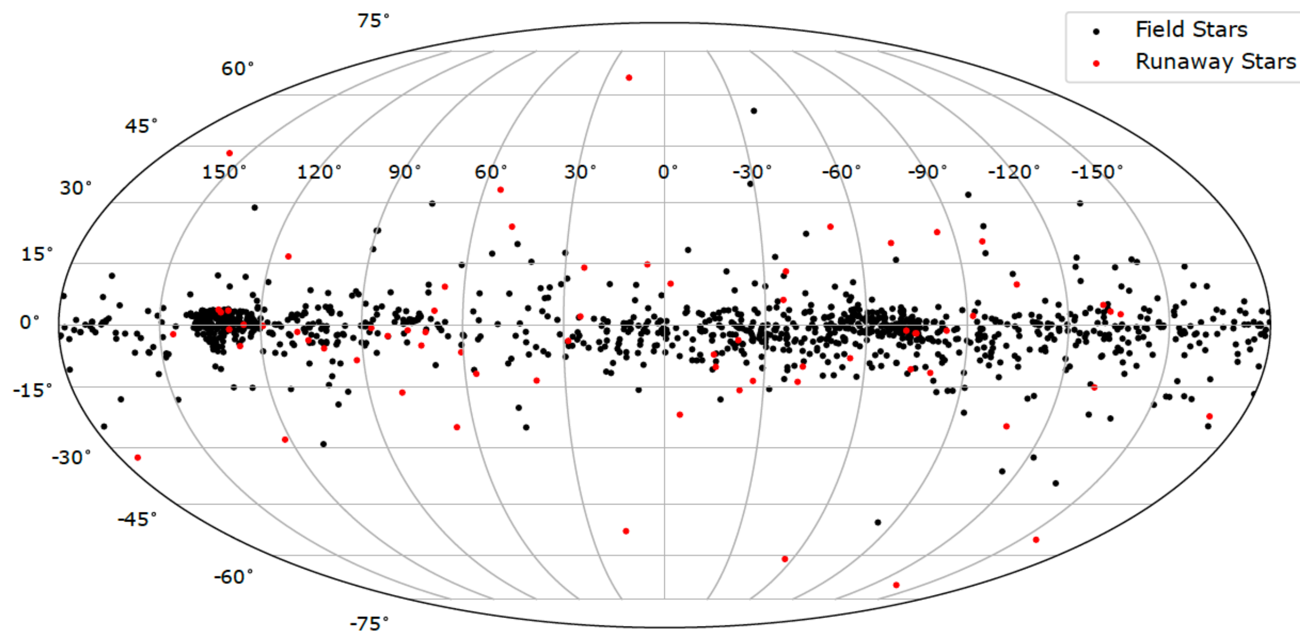

Fig. 13. Galactic (l, b) coordinates for BeSS-*Gaia* DR3 stars. Field stars are depicted in black, and runaway stars are shown in red.

Backup

Table 6. Main characteristics of works on all-sky searches of runaways among young stars discussed in Sect. 6.3.

Sample	Method	Thresholds	Runaways	References
HIPPARCOS and v_r; age $\leq$ 50 Myr; d < 3 kpc	3D velocities	28 km s^{-1}	~27%	Tetzlaff et al. (2011)
GOSC and *Gaia* DR1	2D proper motions	None	~5.7%	Maíz Apellániz et al. (2018)
GOSC and *Gaia* EDR3	2D velocities	25 km s^{-1}	~22%	Kobulnicky & Chick (2022)
GOSC and *Gaia* DR3	2D velocities	None	25.4%	This work
GOSC and *Gaia* DR3	3D velocities (sim.)	None	30.0%	This work
BeSS, *Gaia* DR1 and LAMOST; B&G (2001)	3D velocities	None	~13%	Boubert & Evans (2018)
BeSS and *Gaia* DR3	2D velocities	None	5.2%	This work
BeSS and *Gaia* DR3	3D velocities (sim.)	None	6.7%	This work

Notes. B&G (2001) stands for Berger & Gies (2001). 3D velocities (sim.) stands for simulated 3D velocities (see Appendix D).

Backup

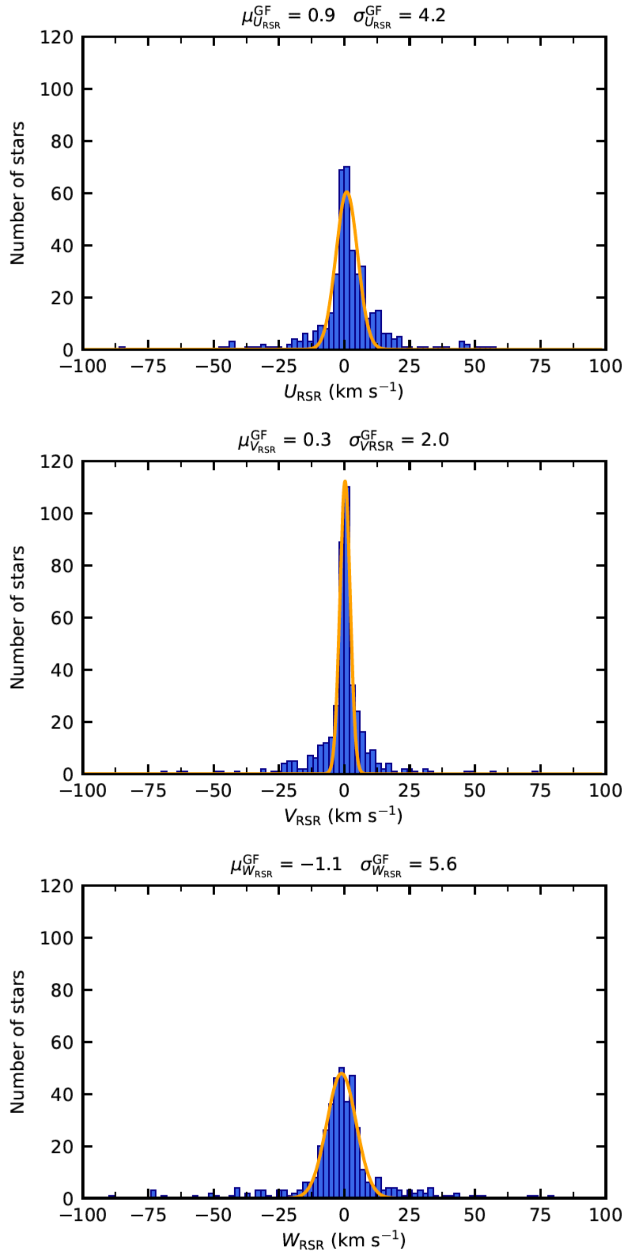

Fig. B.1. Distributions of the U_{RSR}, V_{RSR} , and W_{RSR} velocities for the GOSC-*Gaia* DR3 stars. The histograms have a bin size of 2 km s^{-1}. The orange lines represent Gaussian functions fitted to the data, whose means and standard deviations in km s^{-1} are quoted above the panels. The abscissa ranges have been limited to ±100 km s^{-1}. *Top*: Histogram of the U_{RSR} velocities. *Middle*: Histogram of the V_{RSR} velocities. *Bottom*: Histogram of the W_{RSR} velocities.

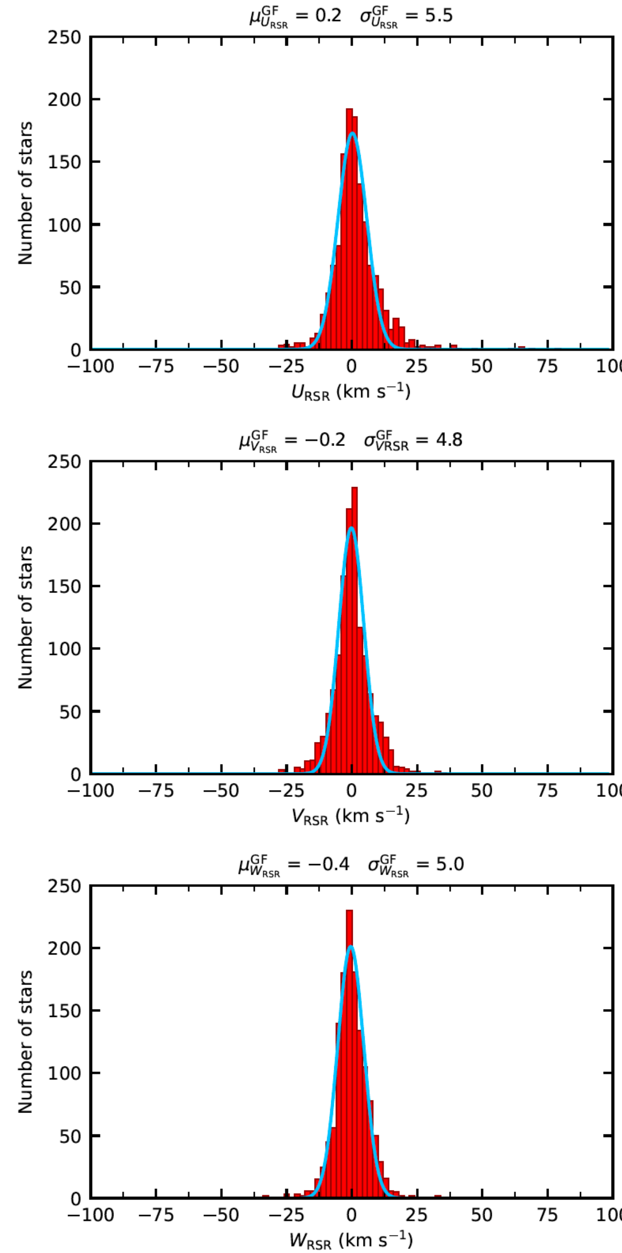

Fig. B.2. Same as Fig. B.1, but for the BeSS-*Gaia* DR3 stars and with the Gaussian functions fitted to the data shown in blue.

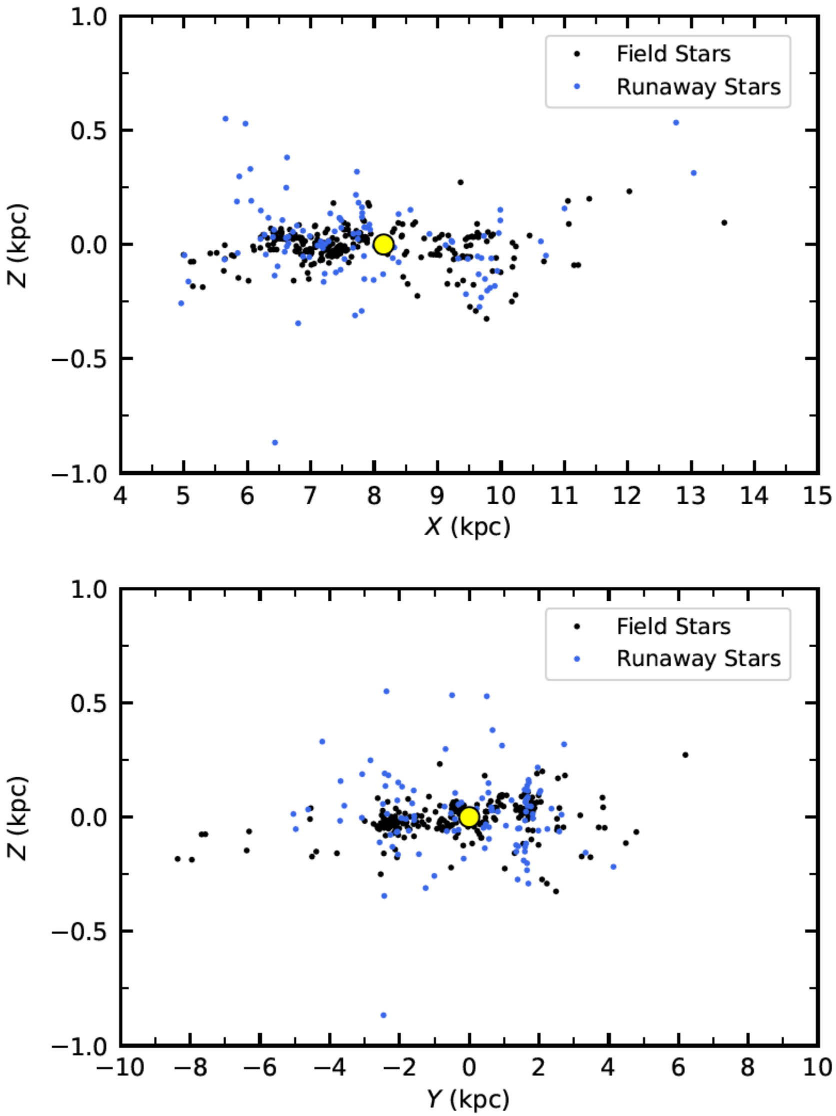

Fig. C.1. Galactocentric *XZ* and *YZ* coordinates for the stars of the GOSC-*Gaia* DR3 catalog. Field stars are depicted in black, and runaway stars are shown in blue. The position of the Sun is marked with a yellow circle. The ordinate axis is limited to ±1 kpc and the axes have different scales. *Top*: Galactocentric *XZ* coordinates. *Bottom*: Galactocentric *YZ* coordinates, but with a different scale in the abscissa axis.

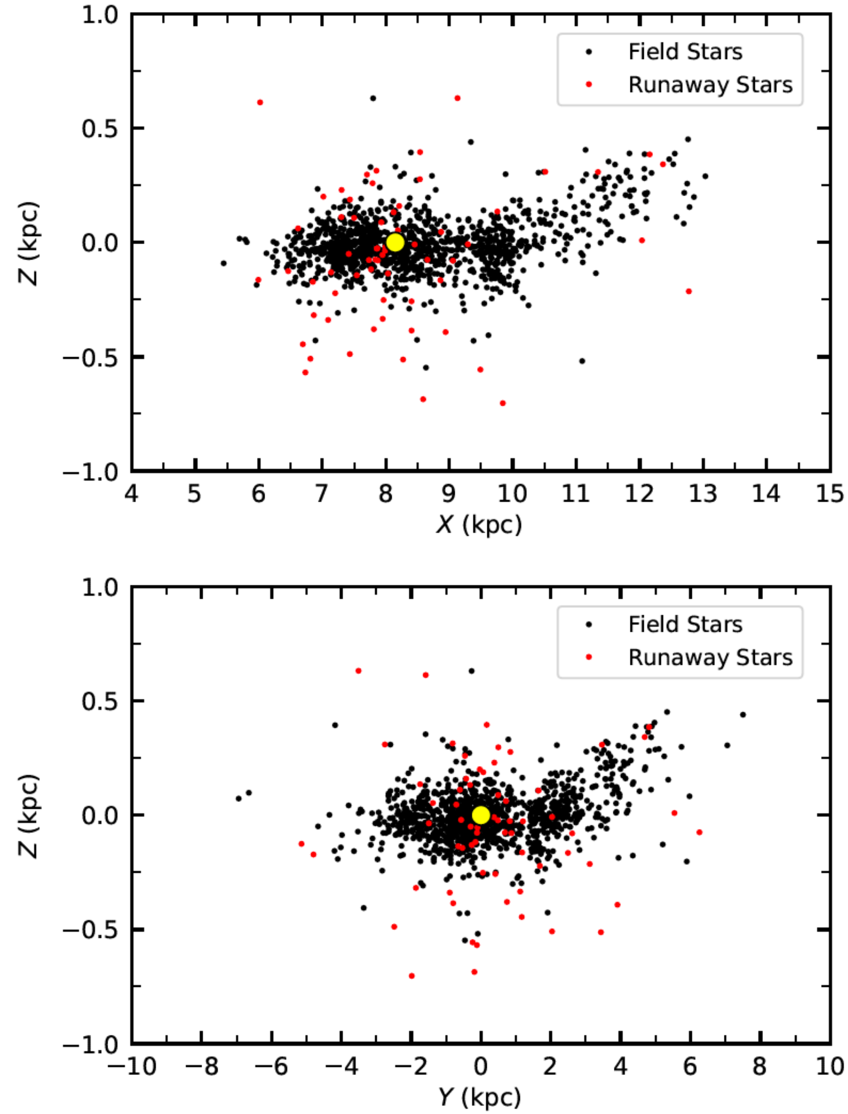

Fig. C.2. Same as Fig. C.1 for the BeSS-*Gaia* DR3 stars. Field stars are depicted in black, and runaway stars are shown in red.

Backup

Table 3. Main properties of the IR and radio surveys used in this work.

Survey	Band	Wavelength	Resolution ($''$)	Coverage	Ref.
WISE	W1	3.4 μm	6.1	All sky	1
	W2	4.6 μm	6.4	All sky	1
	W3	12 μm	6.5	All sky	1
	W4	22 μm	12	All sky	1
NVSS		21 cm	45	$\delta \gtrsim -40°$	2
VLASS		10 cm	2.5	$\delta \gtrsim -40°$	3
RACS	low	34 cm	$\sim$15	$\delta \lesssim +49°$	4
RACS	mid	22 cm	$\sim$10	$\delta \lesssim +49°$	5

References. (1) Wright et al. (2010); (2) Condon et al. (1998); (3) Lacy et al. (2020); (4) Hale et al. (2021); (5) Duchesne et al. (2024).

Backup

Table 4. Stellar parameters and velocities of the runaway stars associated to the new bow shock (BS) and bubble (BU) candidates, and geometrical IR measures in W4 for the bow shock and bubble candidates.

S. T.	$\dot{M} \times 10^6$ ($M_\odot$ yr^{-1})	v_∞ (km s^{-1})	v_r (km s^{-1})	Ref	V^{3D}_{PEC} (km s^{-1})	BS/BU	R ($''$)	R (pc)	l ($''$)	l (pc)	w ($''$)	w (pc)	e	n_{ISM} (cm^{-3})
O7.5V	0.06	3349	−18	1	79.4	BS-GR9	19	0.16	123	1.05	38	0.32	0.51	2.8
O4.5III	1.00	3465	−39	2	51.5	BS-GR34	151	1.22	373	3.00	56	0.45	0.37	2.8
O3V	3.90	4175	77	1	87.0	BS-GR35	91	1.77	357	6.95	34	0.66	0.70	7.1
ON9.7II	0.06	3110	−17	1	42.9	BS-GR71	55	0.63	171	1.96	73	0.84	0.43	0.6
O4V	4.01	3984	−36	2	47.2	BS-GR72	30	0.43	192	2.74	30	0.43	0.18	198.6
O7.5V	0.07	3349	−1.5	3	21.3	BS-GR75	28	0.28	309	3.10	110	1.10	0.47	12.7
O9.5IV	0.07	3157	−27	1	34.6	BU-GR78	–	–	–	–	125	1.03	–	–
O9.7III	0.07	3116	39.9	1	45.1	BS-GR80	20	0.19	175	1.71	90	0.88	0.29	4.9
O7.5Ia	0.05	3268	−39	3	48.0	BS-GR93	32	0.60	225	4.21	101	1.89	0.21	1.4
O5:	–	–	−10.2	3	19.0	BU/BS-GR100	–/13	–/0.20	–/186	–/2.93	69/74	1.09/1.17	–/0.51	–
B0.5eIII	0.05	3044	−18	1	47.9	BU-BR21	–	–	–	–	105	0.99	–	–
B1psheV	0.06	3053	–	–	–	BU-BR46	–	–	–	–	78	0.67	–	–
Be	–	–	–	–	–	BS-BR65	112	0.26	138	0.32	36	0.08	0.71	–

Notes. Left side of the table provides information associated to the runaway stars, while right part provides information associated to the corresponding bow shock and bubble candidates. Spectral types (S. T.) are taken from the GOSC (Maíz Apellániz et al. 2013) and the BeSS (Neiner et al. 2011) catalogs. $\dot{M}$ mass-loss rates were linearly interpolated from Vink & Sander (2021). Wind terminal velocities were obtained applying a linear regression to Vink & Sander (2021) data. Radial velocity references: (1) de Bruijne & Eilers (2012); (2) Kobulnicky & Chick (2022); (3) Kharchenko et al. (2007). V^{3D}_{PEC} is obtained from v_r and the V^{2D}_{PEC} computed in Carretero-Castrillo et al. (2023). Right side of the table provides the classification id of the IR structure around the runaway star: BS for bow shocks; BU for bubbles; BU/BS and BS/BU for intermediate structures between BS and BU. R is projected the stand-off distance from the star to the midpoint of the bow shock, l is the length, and w is the width of the bow shock structure. These distances are projected in the plane of the sky. For bubbles, only the width is measured. Column e provides the eccentricity of the ellipse used to measure the bow shocks. n_{ISM} is the ISM density of the medium around the bow shock position. The horizontal line separates O-type stars (upper part) from Be-type stars (bottom part). This table is available at the CDS.

Backup

Table 6. Miscellaneous IR structures and their W4 morphology.

Run. id	W4 Morph.	Run. id	W4 Morph.	Run. id	W4 Morph.	Run. id	W4 Morph.	Run. id	W4 Morph.	Run. id	W4 Morph.
GR4	•	GR6	•	GR10	•	GR11	•	GR19	•	GR21	•
GR23	•	GR30	•	GR32	•	GR33	•	GR36	•	GR37	•
GR38	⊃	GR41	•	GR43	•	GR46	•	GR47	⊃	GR48	•
GR49	•	GR53	•	GR55	•	GR57	•	GR58	•	GR60	•
GR63	•	GR64	•	GR66	•	GR68	◯	GR69	•	GR74	•
GR79	•	GR81	◯	GR84	•	GR85	•	GR86	•	GR87	•
GR94	•	GR96	•	GR98	•	GR101	⊃				
BR1	•	BR2	•	BR3	•	BR4	•	BR5	•	BR7	•
BR8	•	BR9	•	BR10	∘	BR11	•	BR15	∘	BR16	•
BR20	•	BR27	•	BR28	•	BR29	•	BR30	•	BR32	•
BR34	•	BR37	•	BR45	•	BR58	•				

Notes. Morphology observed in W4 image: ⊃ curved structure; ◯ kind of bubble; • point-like source; ∘ mini-bubble.

Backup

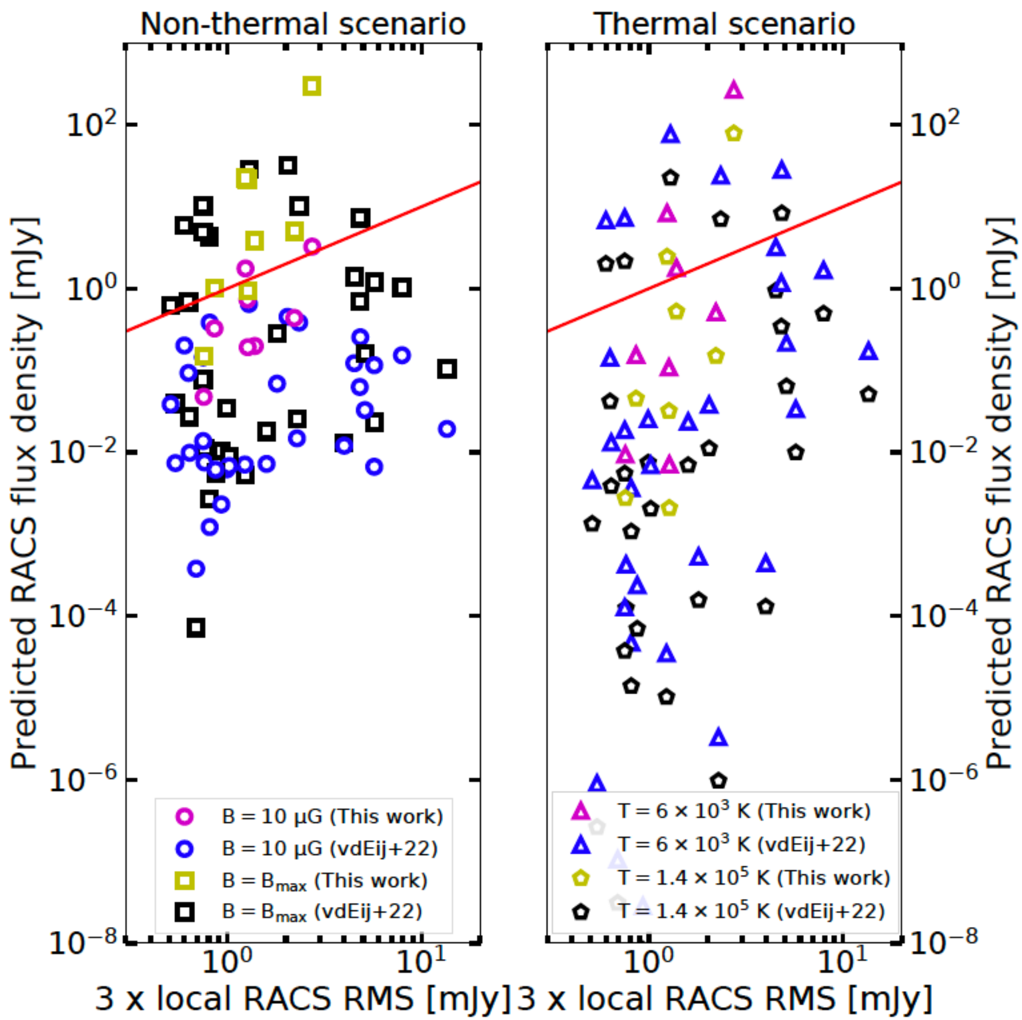

Fig. 7. Predicted peak radio flux density as a function of three times the local RMS for the non-thermal (left) and thermal (right) scenarios. This plot contains the original data presented in van den Eijnden et al. (2022b), and our sources in yellow and magenta colors, with different symbols depending on the scenario conditions. The one-to-one line is shown by the red line; sources above it should, at minimum, have observable emission in a single beam.